Elimination of Computing Singular Surface Integrals in the PIES Method through Regularization for Three-Dimensional Potential Problems

Krzysztof Szerszeń [0000-0001-9256-2622] and Eugeniusz Zieniuk [0000-0002-6395-5096]

University of Bialystok, Faculty of Computer Science
15-245 Białystok, Konstantego Ciołkowskiego 1M, Poland
k.szerszen@uwb.edu.pl, e.zieniuk@uwb.edu.pl

Abstract. We propose a technique to circumvent the direct computation of singular surface integrals in parametric integral equation system (PIES) employed for solving three-dimensional potential problems. It is based on the regularization of the original singular PIES formula, resulting in the simultaneous elimination of both strongly and weakly singular integrals. As a result, there is the possibility of numerically calculating the values of all integrals in the obtained formula using standard Gaussian quadrature. The evaluation of accuracy for the proposed approach is examined through an illustrative case, specifically focusing on the steady-state temperature field distribution problem.

Keywords: Regularized PIES, Singular Integrals, Three-Dimensional Boundary Value Problems, Bézier Surfaces

1 Introduction

Simulation studies typically involve formulating the considered problem as a boundary value problem (BVP) and describing it using partial differential equations (PDEs). Beyond selecting appropriate PDE, it becomes imperative to define the geometric configuration of the computational domain and establish boundary conditions. While formulating a boundary problem may seem relatively simple, obtaining a direct analytical solution is feasible only for a limited set of problems characterized by simple domain shapes and boundary conditions. In the case of practical problems with more complex geometry and complicated boundary conditions, obtaining a solution becomes a task that requires the application of numerical computational methods. Examples of such methods include the finite difference method (FDM) [1], the finite element method (FEM) [2], the boundary element method (BEM) [3] and meshless methods [4].

Parametric integral equatiom system (PIES) is a computational method for solving two and three-dimansional BVPs, where the necessity of subdividing the boundary and domain into conventional finite and boundary elements has been eliminated [5]. This is made possible through the analytical inclusion of the shape of the considered problem directly in the mathematical formula of PIES, along with the introduction of

ICCS Camera Ready Version 2024
To cite this paper please use the final published version:
DOI: 10.1007/978-3-031-63751-3_22

alternative methods to describe this geometry. Particularly promising is the description of the shape of three-dimensional boundary problems using parametric surface patches [6]. Consequently, instead of employing a mesh of boundary elements with declared nodes, which is characteristic of BEM, the shape of the boundary in the PIES can be defined using a smaller number of parametric surface patches, determined by a relatively small set of control points.

One of the primary challenges encountered in PIES is the computation of weakly and strongly singular integrals. Their presence results from the fact that PIES is an analytical modification of boundary integral equations (BIEs). This modification, previously employed in various differential equation contexts [5,6], is designed to analytically account for the shape of the boundary problem without the necessity of using elements. PIES transforms the considered problem, originally described by its corresponding differential equation as a boundary-based problem in the case of BIEs, into a parameterized reference domain that maps this boundary. In 2D problems, this involves integrating along a parameterized straight line corresponding to the parameterized boundary contour, and in 3D problems, it requires integration over a two-dimensional parameterized plane representing the boundary surface.

Recognizing the importance of computing singular integrals, a substantial body of literature has been devoted to thoroughly addressing and advancing this subject. These methods are largely dedicated to BEM, among which we can mention adaptive element subdivision [7], distance transformation [8], variable transformation [9], polar coordinate transformation [10], analytical and semi-analytical methods [11-12], and quadrature methods [13]. One of the most promising approaches is regularization methods [14-16].

The paper presents a regularization technique for PIES in 3D problems, aiming to eliminate both weak and strong singularities. This approach extends a previous regularization method developed for 2D problems [17-19]. The proposed method involves regularization of the original singular PIES formula by introducing an auxiliary regularization functions, incorporating unknown coefficients, and applying appropriate transformations. The effectiveness of this strategy is demonstrated through the analysis of the steady-state temperature field distribution governed by Laplace's equation.

2 PIES for the Laplace equation in 3D and its numerical solution

We consider the analysis of the steady-state temperature field within a three-dimensional domain Ω bounded by the boundary Γ. Mathematically, the problem is described as a boundary value problem for the Laplace equation

$$\frac{\partial^2 u}{\partial x_1^2} + \frac{\partial^2 u}{\partial x_2^2} + \frac{\partial^2 u}{\partial x_3^2} = 0, \tag{1}$$

with prescribed Dirichlet boundary conditions u_Γ and Neumann conditions p_Γ. In the case of practical problems related to more complex shapes of the domain, such as the one illustrated in Figure 1a, computational methods are employed to determine the

ICCS Camera Ready Version 2024
To cite this paper please use the final published version:
DOI: 10.1007/978-3-031-63751-3_22

temperature field distribution. Figure 1b illustrates the boundary element modeling of the boundary Γ, commonly used in BEM. A similar discretization strategy applies to FEM, but it is confined to the domain defined by finite elements. While such modeling has gained popularity, it often results in a large number of elements and a substantial size of algebraic equations to be solved in practice.

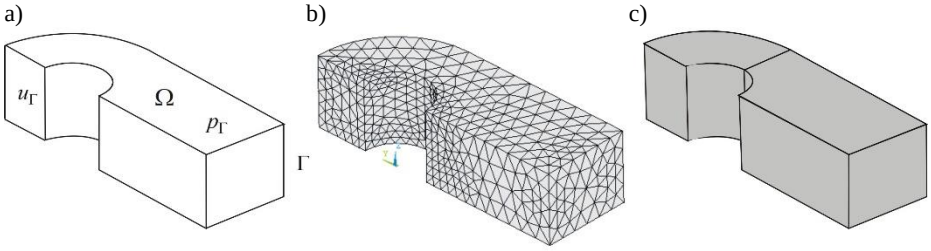

Fig. 1. Sample domain Ω with corresponding boundary conditions (a), discretization of the boundary using boundary elements in BEM (b), an alternative representation of the boundary with surface patches in PIES (c).

To overcome the limitations of FEM and BEM, the PIES method can be employed, enabling a mathematical simplification of the problem by one dimension. Analogous to BIE, the field within the domain Ω is determined by analyzing the boundary Γ of this domain. However, PIES introduces an analytical modification of BIE, transforming the problem from being directly defined on the boundary to one defined on a parameterized reference domain. In the case of 3D problems, this entails mapping the boundary of the problem onto a parameterized plane. A visual representation of this process can be found in Figure 2.

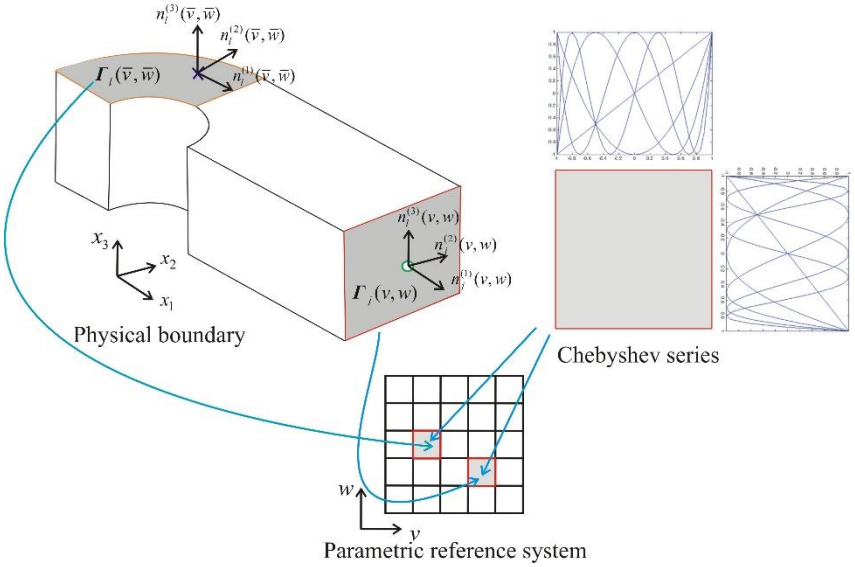

Fig. 2. Mapping of the boundary Γ onto a parameterized plane with the approximation of boundary functions Chebyshev series.

ICCS Camera Ready Version 2024
To cite this paper please use the final published version:
DOI: 10.1007/978-3-031-63751-3_22

The presented approach allows for a general description of the boundary using various mathematical functions. By $\boldsymbol{\Gamma}_j(v,w)$, we define a general parameterized function dependent on parameters v and w from the parameterized reference plane, describing the shape of the j-th segment of the boundary. These functions are analytically integrated into the PIES formula, which, for Laplace's equation, is expressed as [5]

$$0.5u_l(\bar{v},\bar{w}) = \sum_{j=1}^{N}\int_{v_{j-1}}^{v_j}\int_{w_{j-1}}^{w_j}\{\bar{U}_{lj}^*(\bar{v},\bar{w},v,w)p_j(v,w) - \bar{P}_{lj}^*(\bar{v},\bar{w},v,w)u_j(v,w)\}J_j(v,w)dvdw, \tag{2}$$

where $v_{j-1} < \bar{v}, v < v_j, w_{j-1} < \bar{w}, w < w_j, l = 1,2,3,\ldots,n.$

Compared to BIE, the sub-integral functions $\bar{U}_{lj}^*(\bar{v},\bar{w},v,w)$ and $\bar{P}_{lj}^*(\bar{v},\bar{w},v,w)$ from formula (2) are not directly defined on the boundary but within the parameterized domain of $\boldsymbol{\Gamma}_j(v,w)$. For the Laplace equation, they are defined as follows

$$\bar{U}_{lj}^*(\bar{v},\bar{w},v,w) = \frac{1}{4\pi}\frac{1}{(\eta_1^2+\eta_2^2+\eta_3^2)^{0.5}}, \tag{3}$$

$$\bar{P}_{lj}^*(\bar{v},\bar{w},v,w) = \frac{1}{4\pi}\frac{\eta_1 n_j^{(1)}(v,w)+\eta_2 n_j^{(2)}(v,w)++\eta_3 n_j^{(3)}(v,w)}{(\eta_1^2+\eta_2^2+\eta_3^2)^{1.5}}, \tag{4}$$

where

$$\eta_1 = \Gamma_l^{(1)}(\bar{v},\bar{w}) - \Gamma_j^{(1)}(v,w), \eta_2 = \Gamma_l^{(2)}(\bar{v},\bar{w}) - \Gamma_j^{(2)}(v,w),$$
$$\eta_3 = \Gamma_l^{(2)}(\bar{v},\bar{w}) - \Gamma_j^{(3)}(v,w), \tag{5}$$

where $\Gamma_j^{(1)}$, $\Gamma_j^{(2)}$ and $\Gamma_j^{(3)}$ are the scalar components of the function $\boldsymbol{\Gamma}_j(v,w)$. Additionally, $n_j^{(1)}$, $n_j^{(2)}$ and $n_j^{(3)}$ denote the normal derivatives to the boundary, while $J_j(v,w)$ represents the Jacobian of the mapping between the Cartesian coordinate system and the parameterized reference plane dependent on parameters v and w. Formula (2) eliminates the need to use boundary elements to describe the shape of the boundary, as is the case in BEM, which is a numerical implementation of BIEs. In this work, we employ parametric Bézier surfaces for $\boldsymbol{\Gamma}_j(v,w)$. Figure 1c illustrates the definition of the boundary, showcasing an example that utilizes six first-degree and seven third-degree Bézier surface patches.

PIES also allows for the separation of the boundary declaration, defined by $\boldsymbol{\Gamma}_j(v,w)$, from the approximation on this boundary of the boundary functions denoted in equation (2) by $u_j(v,w)$ and $p_j(v,w)$. Boundary functions may take a different form than the functions $\boldsymbol{\Gamma}_j(v,w)$. In this context, we assume that the boundary functions on each Bézier surface denoted by by j are expressed as Chebyshev series, taking the following form

$$u_j(v,w) = \sum_{p=0}^{P-1}\sum_{r=0}^{R-1} u_j^{(pr)} T_j^{(p)}(v) T_j^{(r)}(w), \tag{6}$$

$$p_j(v,w) = \sum_{p=0}^{P-1}\sum_{r=0}^{R-1} p_j^{(pr)} T_j^{(p)}(v) T_j^{(r)}(w), \tag{7}$$

ICCS Camera Ready Version 2024
To cite this paper please use the final published version:
DOI: 10.1007/978-3-031-63751-3_22

where $u_j^{(pr)}$ and $p_j^{(pr)}$ represent the values of successive coefficients in these series. Separating the approximation of boundary functions from the declaration of the boundary shape provides control over the accuracy of solutions obtained on the boundary without affecting the pre-defined functions $\boldsymbol{\Gamma}_j(v,w)$ characterizing the boundary shape. When utilizing Chebyshev series, accuracy improvement is achieved by increasing the number of terms, denoted by P and R. This approach contrasts with BEM, where the same boundary elements both model the boundary shape and determine the field distribution on the boundary, necessitating a re-discretization of the boundary shape when increasing the number of elements to enhance accuracy in boundary solutions.

3 Elimination of singulatities from PIES through regularization

In the case where $l = j$ and $v \to \bar{v}$, $w \to \bar{w}$, the sub-integral function $\bar{U}_{lj}^*(\bar{v},\bar{w},v,w)$ is weakly singular, while $\bar{P}_{lj}^*(\bar{v},\bar{w},v,w)$ is strongly singular. Utilizing Gaussian quadrature directly for computing integrals in formula (2), without isolating singular points, leads to significant errors that directly impact the accuracy of the solutions. The aim of this study is to eliminate singularities from this formula through regularization. To achieve this, in the first step of the proposed procedure, we rewrite (2) with a modified form of boundary functions, denoted as $\breve{u}_j(v,w)$ and $\breve{p}_j(v,w)$, which is presented as

$$0.5\breve{u}_l(\bar{v},\bar{w}) = \sum_{j=1}^{N}\int_{v_{j-1}}^{v_j}\int_{w_{j-1}}^{w_j}\left\{\bar{U}_{lj}^*(\bar{v},\bar{w},v,w)\breve{p}_j(v,w) - \bar{P}_{lj}^*(\bar{v},\bar{w},v,w)\breve{u}_j(v,w)\right\}J_j(v,w)dvdw. \tag{8}$$

In our considerations, we assume that $\breve{u}_j(v,w)$ takes the following form

$$\breve{u}_j(v,w) = A_l(\bar{v},\bar{w})\left[\left(\Gamma_l^{(1)}(\bar{v},\bar{w}) - \Gamma_j^{(1)}(v,w) + \Gamma_l^{(2)}(\bar{v},\bar{w}) - \Gamma_j^{(2)}(v,w) + \Gamma_l^{(3)}(\bar{v},\bar{w}) - \Gamma_j^{(3)}(v,w)\right] + B_l(\bar{v},\bar{w}), \tag{9}$$

along with its directional derivative with respect to the normal vector to the boundary, in the form

$$\breve{p}_j(v,w) = A_l(\bar{v},\bar{w})\left[n_j^{(1)}(v,w) + n_j^{(2)}(v,w) + n_j^{(3)}(v,w)\right], \tag{10}$$

where $A_l(\bar{v},\bar{w})$ and $B_l(\bar{v},\bar{w})$ represent regularization coefficients defined as

$$A_l(\bar{v},\bar{w}) = \frac{p_j(v,w)}{n_l^{(1)}(\bar{v},\bar{w}) + n_l^{(2)}(\bar{v},\bar{w}) + n_l^{(3)}(\bar{v},\bar{w})}, \tag{11}$$

$$B_l(\bar{v},\bar{w}) = u_l(\bar{v},\bar{w}). \tag{12}$$

The functions (11, 12) are selected to satisfy the Laplace equation. By subtracting (8) from (2), the final formula for the regularized PIES is derived

ICCS Camera Ready Version 2024
To cite this paper please use the final published version:
DOI: 10.1007/978-3-031-63751-3_22

$$\sum_{j=1}^{N}\Big\{\int_{v_{j-1}}^{v_j}\int_{w_{j-1}}^{w_j}\bar{U}_{lj}^{*}(\bar{v},\bar{w},v,w)\big[p_j(v,w)-d_{lj}(\bar{v},\bar{w},v,w)p_l(\bar{v},\bar{w})\big]- \int_{v_{j-1}}^{v_j}\int_{w_{j-1}}^{w_j}\bar{P}_{lj}^{*}(\bar{v},\bar{w},v,w)[u_j(v,w)-u_l(\bar{v},\bar{w})- g_{lj}(\bar{v},\bar{w},v,w)p_l(\bar{v},\bar{w})]\Big\}J_j(v,w)dvdw=0, \tag{13}$$

where

$$d_{lj}(\bar{v},\bar{w},v,w)=\frac{n_j^{(1)}(v,w)+n_j^{(2)}(v,w)+n_j^{(3)}(v,w)}{n_l^{(1)}(\bar{v},\bar{w})+n_l^{(2)}(\bar{v},\bar{w})+n_l^{(3)}(\bar{v},\bar{w})}, \tag{14}$$

$$g_{lj}(\bar{v},\bar{w},v,w)=\frac{(\Gamma_j^{(1)}(v,w)-\Gamma_l^{(1)}(\bar{v},\bar{w}))+(\Gamma_j^{(2)}(v,w)-\Gamma_l^{(2)}(\bar{v},\bar{w}))+(\Gamma_j^{(3)}(v,w)-\Gamma_l^{(3)}(\bar{v},\bar{w}))}{n_l^{(1)}(\bar{v},\bar{w})+n_l^{(2)}(\bar{v},\bar{w})+n_l^{(3)}(\bar{v},\bar{w})}. \tag{15}$$

The use of functions $d_{lj}(\bar{v},\bar{w},v,w)$ and $g_{lj}(\bar{v},\bar{w},v,w)$ eliminates the presence of weak and strong singularities. To find the solution for the formula (13), the collocation method can be employed. Collocation points are be distributed in the parametric domain of PIES and defined by the parameter values $\bar{v}$ and $\bar{w}$. Evaluating (13) at the collocation points will yield a system of algebraic equations which can be expressed in general terms as

$$[G]\{u\}=[H]\{p\}. \tag{16}$$

Its size depends on the number of Bézier patches modeling the boundary and the number of terms in the Chebyshev approximation series. The off-diagonal elements in (16) are determined based on the following non-singular integrals

$$\big[g_{lj}^{(c,d,p,r)}\big]=\int_{v_{j-1}}^{v_j}\int_{w_{j-1}}^{w_j}\bar{P}_{lj}^{*}\big(\bar{v}^{(c,d)},\bar{w}^{(c,d)},v,w\big)T_j^{(p)}(v)T_j^{(r)}(w)J_j(v,w)dvdw, \tag{17}$$

$$\big[h_{lj}^{(c,d,p,r)}\big]=\int_{v_{j-1}}^{v_j}\int_{w_{j-1}}^{w_j}\bar{U}_{lj}^{*}\big(\bar{v}^{(c,d)},\bar{w}^{(c,d)},v,w\big)T_j^{(p)}(v)T_j^{(r)}(w)J_j(v,w)dvdw. \tag{18}$$

The practical application of the presented regularization relies on the introduction of auxiliary matrices $[\tilde{G}]$, $[\hat{G}]$, $[\tilde{H}]$ incorporating regularization functions (14) and (15)

$$\big[G-diag\{\textstyle\sum_{row}[\tilde{G}]\}\big]\{u\}=\big[H-diag\{\textstyle\sum_{row}[\tilde{H}]\}-diag\{\textstyle\sum_{row}[\hat{G}]\}\big]\{p\}. \tag{19}$$

The elements of the matrices $[\tilde{G}]$, $[\hat{G}]$, $[\tilde{H}]$ are as follows

$$\big[\tilde{g}_{ll}^{(c,d,p,r)}\big]=\int_{v_{j-1}}^{v_j}\int_{w_{j-1}}^{w_j}\bar{P}_{lj}^{*}\big(\bar{v}^{(c,d)},\bar{w}^{(c,d)},v,w\big)T_j^{(p)}(v)T_j^{(r)}(w)J_j(v,w)dvdw, \tag{20}$$

$$\big[\hat{g}_{ll}^{(c,d,p,r)}\big]=\int_{v_{j-1}}^{v_j}\int_{w_{j-1}}^{w_j}\frac{(\Gamma_j^{(1)}(v,w)-\Gamma_l^{(1)}(\bar{v},\bar{w}))+(\Gamma_j^{(2)}(v,w)-\Gamma_l^{(2)}(\bar{v},\bar{w}))+((\Gamma_j^{(3)}(v,w)-\Gamma_l^{(3)}(\bar{v},\bar{w}))}{n_l^{(1)}(\bar{v}^{(c,d)},\bar{w}^{(c,d)})+n_l^{(2)}(\bar{v}^{(c,d)},\bar{w}^{(c,d)})+n_l^{(3)}(\bar{v}^{(c,d)},\bar{w}^{(c,d)})}*$$
$$\bar{P}_{jl}^{*}\big(\bar{v}^{(c,d)},\bar{w}^{(c,d)},v,w\big)T_j^{(p)}(v)T_j^{(r)}(w)J_j(v,w)dvdw, \tag{21}$$

$$\big[\hat{h}_{ll}^{(c,d,p,r)}\big]=\int_{v_{j-1}}^{v_j}\int_{w_{j-1}}^{w_j}\frac{n_j^{(1)}(v,w)+n_j^{(2)}(v,w)+n_j^{(3)}(v,w)}{n_l^{(1)}(\bar{v}^{(c,d)},\bar{w}^{(c,d)})+n_l^{(2)}(\bar{v}^{(c,d)},\bar{w}^{(c,d)})+n_l^{(3)}(\bar{v}^{(c,d)},\bar{w}^{(c,d)})}*$$

ICCS Camera Ready Version 2024
To cite this paper please use the final published version:
DOI: 10.1007/978-3-031-63751-3_22

$$\bar{U}_{jl}^{*}\left(\bar{v}^{(c,d)},\bar{w}^{(c,d)},v,w\right)T_j^{(p)}(v)T_j^{(r)}(w)J_j(v,w)dvdw. \tag{22}$$

All integrals in (19) can be numerically computed through standard Gaussian quadrature. The comprehensive algorithm for solving the regularized PIES is presented below.

Algorithm for Regularized PIES

Read boundary input data (control points of n Bézier surfaces), **Read boundary conditions**
for $l \leftarrow 1, N$ **do** *//loop over Bézier surfaces*
for $j \leftarrow 1, N$ **do**
if $l == j$ **then**
for $p \leftarrow 0, P-1$ **do** *//loop over Chebyshev series*
for $r \leftarrow 0, R-1$ **do**
for $c \leftarrow 0, C-1$ **do** *//loop over collocation points*
for $d \leftarrow 1, D-1$ **do**
for $e \leftarrow 1, N$ **do** *//loop over Bézier surfaces*

$$\left[g_{ll}^{(c,d,p,r)}\right] \leftarrow int[\bar{P}_{ll}^{*}\left(\bar{v}^{(c,d)},\bar{w}^{(c,d)},v,w\right)T_l^{(p)}(v)T_l^{(r)}(w)J_l(v,w) - \bar{P}_{le}^{*}\left(\bar{v}^{(c,d)},\bar{w}^{(c,d)},v,w\right)T_e^{(p)}(v)T_e^{(r)}(w)J_e(v,w)]$$

$$\left[h_{ll}^{(c,d,p,r)}\right] \leftarrow int[\bar{U}_{ll}^{*}\left(\bar{v}^{(c,d)},\bar{w}^{(c,d)},v,w\right)T_l^{(p)}(v)T_l^{(r)}(w)J_l(v,w) - \frac{\Gamma_e^{(1)}(v,w)-\Gamma_l^{(1)}(\bar{v},\bar{w})+\Gamma_e^{(2)}(v,w)-\Gamma_l^{(2)}(\bar{v},\bar{w})+\Gamma_e^{(3)}(v,w)-\Gamma_l^{(3)}(\bar{v},\bar{w})}{n_l^{(1)}(\bar{v}^{(c,d)},\bar{w}^{(c,d)})+n_l^{(2)}(\bar{v}^{(c,d)},\bar{w}^{(c,d)})+n_l^{(3)}(\bar{v}^{(c,d)},\bar{w}^{(c,d)})}\bar{P}_{le}^{*}\left(\bar{v}^{(c,d)},\bar{w}^{(c,d)},v,w\right)T_e^{(p)}(v)T_e^{(r)}(w)J_e(v,w) - \frac{n_e^{(1)}(v,w)+n_e^{(2)}(v,w)+n_e^{(3)}(v,w)}{n_l^{(1)}(\bar{v}^{(c,d)},\bar{w}^{(c,d)})+n_l^{(2)}(\bar{v}^{(c,d)},\bar{w}^{(c,d)})+n_l^{(3)}(\bar{v}^{(c,d)},\bar{w}^{(c,d)})}\bar{U}_{le}^{*}\left(\bar{v}^{(c,d)},\bar{w}^{(c,d)},v,w\right)T_e^{(p)}(v)T_e^{(r)}(w)J_e(v,w)]$$

end for
end for
end for
end for
end for
insert submatrix $\left[g_{ll}^{(c,d,p,r)}\right]$ to $\left[g_{ll}\right]$ and $\left[h_{ll}^{(c,d,p,r)}\right]$ to $\left[h_{ll}\right]$
else
for $p \leftarrow 0, P-1$ **do** *//loop over Chebyshev series*
for $r \leftarrow 0, R-1$ **do**
for $c \leftarrow 0, C-1$ **do** *// loop over collocation points*
for $d \leftarrow 1, D-1$ **do**

$$\left[g_{lj}^{(c,d,p,r)}\right] \leftarrow int[\bar{P}_{lj}^{*}\left(\bar{v}^{(c,d)},\bar{w}^{(c,d)},v,w\right)T_j^{(p)}(v)T_j^{(r)}(w)J_j(v,w)]$$

$$\left[h_{lj}^{(c,d,p,r)}\right] \leftarrow int[\bar{U}_{lj}^{*}\left(\bar{v}^{(c,d)},\bar{w}^{(c,d)},v,w\right)T_j^{(p)}(v)T_j^{(r)}(w)J_j(v,w)]$$

end for
end for
end for
end for
insert submatrix $\left[g_{lj}^{(c,d,p,r)}\right]$ to $\left[g_{lj}\right]$ and $\left[h_{lj}^{(c,d,p,r)}\right]$ to $\left[h_{lj}\right]$
end if
end for
end for
transform $[\boldsymbol{H}]\{\boldsymbol{u}\} = [\boldsymbol{G}]\{\boldsymbol{p}\}$ into $[\boldsymbol{A}]\{\boldsymbol{x}\} = \{\boldsymbol{b}\}$**,** solve system of equations $[\boldsymbol{A}]\{\boldsymbol{x}\} = \{\boldsymbol{b}\}$

ICCS Camera Ready Version 2024
To cite this paper please use the final published version:
DOI: 10.1007/978-3-031-63751-3_22

4 Numerical examples

The proposed approach is validated through examples featuring analytical solutions. Specifically, the investigation focuses on evaluating the impact of the relative positioning of collocation points and quadrature nodes on the accuracy of solutions.

4.1 Example 1

We consider the problem of temperature distribution in the domain depicted in Figure 3, with the boundary modeled using 6 Bézier patches. Among them, 5 are degree-1 patches defined by 4 corner points each, and one is a degree-3 patch defined by 16 control points, allowing for the specification of the upper curvilinear part of the boundary. It is assumed that the expected temperature field distribution on the boundary and in the domain would be defined by the following analytical function, dependent on Cartesian coordinates and satisfying Laplace's equation

$$u(x_1, x_2, x_3) = {x_1}^2 + x_2 - {x_3}^2. \tag{23}$$

Based on this function, Dirichlet conditions are specified on each surface patch defining the boundary. Additionally, the normal derivative of this function with respect to the boundary in the form of

$$\frac{\partial u(x_1,x_2,x_3)}{\partial n} = 2x_1 n_1 + n_2 - 2x_3 n_3, \tag{24}$$

represents the analytical solution on the boundary.

To utilize equations (2) and (13) for simulating a stationary temperature field, we apply the collocation method. Collocation points are positioned within the parametric domain of individual Bézier surfaces and are represented by points $\bar{v}, \bar{w}$. By expressing equations (2) and (13) at these collocation points, we derive a system of algebraic equations that approximate the PIES. The size of this system is determined by the number of parametric surfaces modeling the boundary and the number of terms in the approximating series (6,7) on individual surface patches.

To find solutions on the boundary, 5×5 collocation points are specified, arranged according to the distribution of roots of Chebyshev polynomials of the second kind. In turn, for numerical integration, a Gauss quadrature of degree 25×25 are applied per Bézier parch, and its nodes are distributed in the same parametric domain. The parameterization of the boundary in PIES allows flexibility in positioning both collocation points and quadrature nodes, identified respectively by $\bar{v}, \bar{w}$ and v, w.

Below, we explore two algorithms for evaluating singular integrals in PIES:

- Isolation of singularities in weakly and strongly singular integrals using G-L quadratures, referred to as isolation;
- The proposed regularization, known as non-singular.

In all instances, non-singular integrals are computed using G-L quadrature. As previously mentioned, the proposed regularization employs standard G-L quadrature, with the quadrature nodes uniformly distributed along all boundary segments. This streamlines the node generation process, which may otherwise become recursive.

ICCS Camera Ready Version 2024
To cite this paper please use the final published version:
DOI: 10.1007/978-3-031-63751-3_22

While higher-degree quadrature can enhance precision, it comes at the cost of increased computational time, as demonstrated in the latter part of the example.

The second algorithm, which isolates singularities, also relies on G-L quadrature. However, it necessitates dividing the integration interval containing singular points into subintervals. This substantially complicates the integration process and necessitates two distinct quadrature distributions for boundary segments housing regular and singular integrals, respectively.

In the case of applying formula (2) to calculate the integral where the collocation point is treated as a singular point, it is common to isolate this point, as illustrated in Figure 3a.

a)

b)

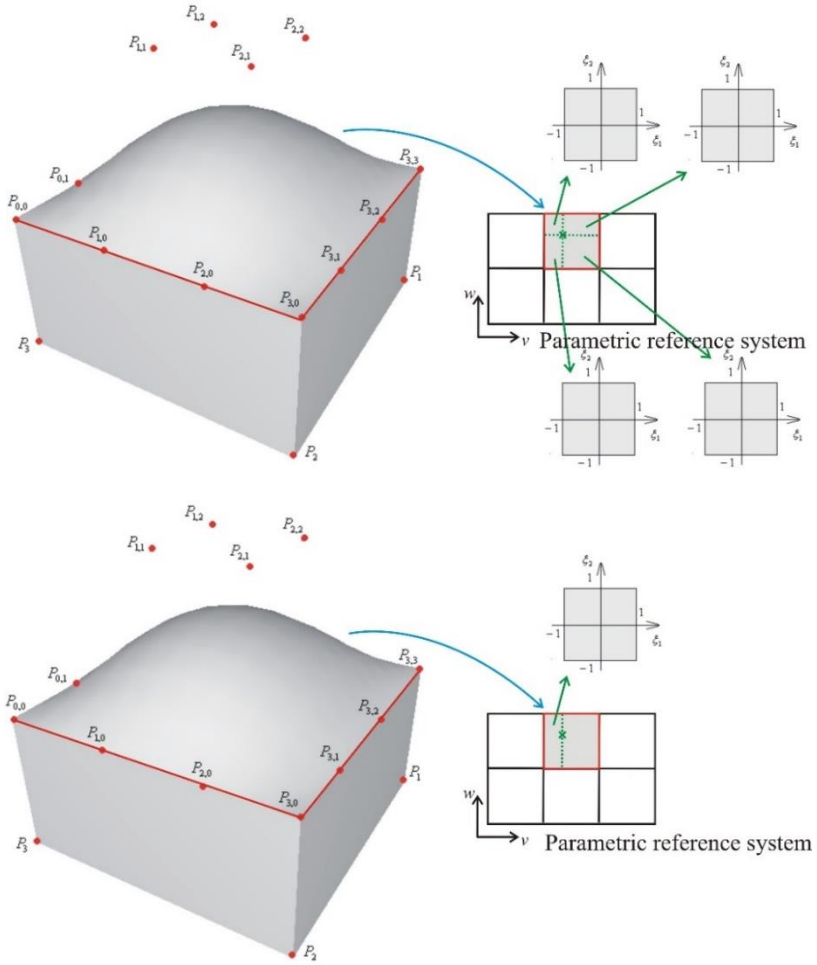

Fig. 3. Mapping of the boundary Γ of the problem onto a parameterized plane with isolating the singular point (a), in the context of the proposed regularization without the need for isolation (b).

ICCS Camera Ready Version 2024
To cite this paper please use the final published version:
DOI: 10.1007/978-3-031-63751-3_22

In this case, for each Bézier surface, we need to isolate each colocation point by dividing the integration domain into four sections and applying independent Gaussian quadrature to each of them. The drawback of this approach is the necessity to modify the integration intervals for each collocation point. In Figure 4a,b, two exemplary divisions are presented for two of the considered 5×5 collocation points, where 25×25 Gaussian quadratures were applied for each of the 4 integration intervals. As we can see in this case, we have an uneven distribution of Gaussian quadrature nodes. On the other hand, applying a varying number of quadrature points tailored to the sizes of the four sub-intervals requires additional intervention in the computational program.

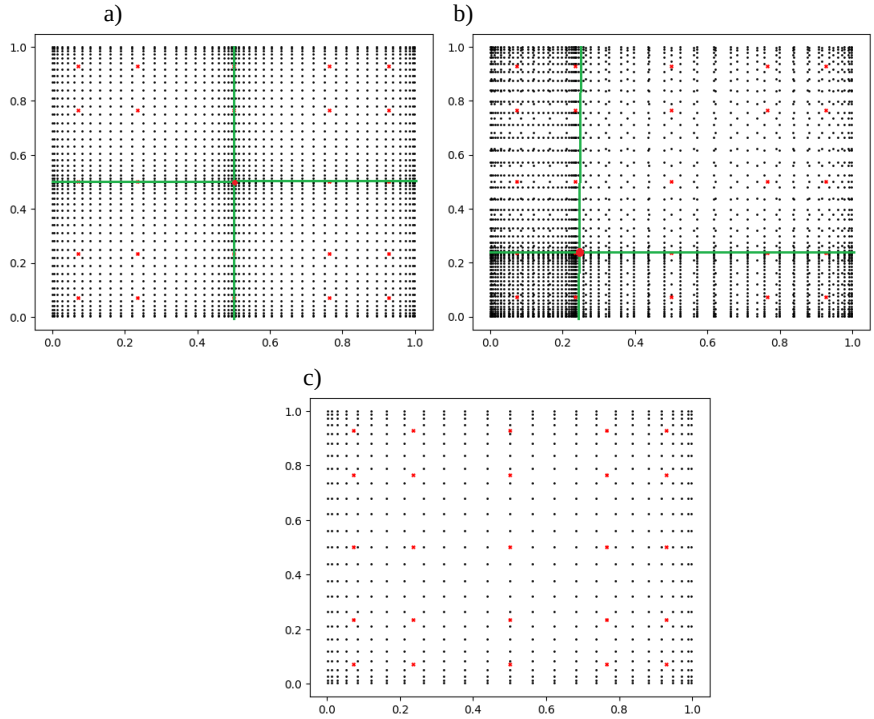

Fig. 4. Two selected distributions of nodes for a 25×25 Gaussian quadrature when dividing the integration domain into 4 parts during the isolation of collocation points $\bar{v}, \bar{w}$, with coordinates (0.5, 0.5) (a) and (0.27, 0.27) (b), in the context of the proposed regularization without the need for isolation (c).

When employing the regularized formula (13), isolation is unnecessary, as depicted in Figure 3b. In this scenario, both collocation points and numerical integration quadrature nodes are within the same interval in the parametric domain of each Bézier patch. This observation is further illustrated in Figure 4c, showcasing a representative configuration of 5×5 and Gauss quadrature 25×25, without the need to subdivide integration intervals. In Table 1, we investigate how the distance between collocation points and quadrature node points affects the accuracy of boundary solutions.

ICCS Camera Ready Version 2024
To cite this paper please use the final published version:
DOI: 10.1007/978-3-031-63751-3_22

Table 1. Influence of the distance between collocation points and Gauss quadrature node on the accuracy of solutions at the boundary.

The coordinates of the central collocation point $\bar{v} = \bar{w}$	The distance between the collocation point and the nearest quadrature node	L_2 norm of the error of solutions at the boundary of the problem (compared to (24))
0.501	1e-3	0.029273
0.5001	1e-4	0.023153
0.50001	1e-5	0.023221
0.500001	1e-6	0.023234
0.5000001	1e-7	0.023197
0.50000001	1e-8	0.146456
0.500000001	1e-9	0.147884

The results from Table 1 indicate the stability of obtained solutions at the boundary depending on the different distances between the positions of quadrature nodes and collocation points. The presented results refer to the vicinity of one selected point among the total of 25 defined. For the remaining points, the presented dependencies are analogous. The obtained results demonstrate the agreement with analytical solutions (24), confirming the effectiveness of the applied strategy.

4.2 Example 2

In the second example, we conducted an analysis of solution accuracy by varying the number of specified collocation points and Gauss quadrature points. The study focused on the domain depicted in Figure 1a, with the boundary defined by 6 Bézier patches of degree 1 and 7 patches of degree 3. Specifying the shape of these patches involved specifying 112 control points. Dirichlet boundary conditions are imposed on the entire boundary and are defined based on the following function

$$u(x_1, x_2, x_3) = {x_1}^3 + 2{x_2}^3 + 3{x_3}^3 - 3x_1{x_3}^2 - 6x_2{x_1}^2 - 9x_3{x_2}^2. \tag{25}$$

Meanwhile, the normal derivative of (25) represents the analytical solution at the boundary of this problem

$$\frac{\partial u(x_1,x_2,x_3)}{\partial n} = n_1(3{x_1}^2 - 3{x_3}^2 - 12x_2x_1) + n_2(6{x_2}^2 - 6{x_1}^2 - 18x_3x_2) + n_3(9{x_3}^2 - 6x_1x_3 - 9{x_2}^2). \tag{26}$$

In the analysis, the number of collocation points is varied from 2×2 to 5×5, while the number of Gauss quadrature nodes is set at 30×30 and 40×40 assigned to each Bézier patches. Similar to example 1, the application of formula (13) does not necessitate the isolation of a singular point. Figure 5 illustrates two exemplary combinations of collocation points and quadrature nodes that are under examination.

ICCS Camera Ready Version 2024
To cite this paper please use the final published version:
DOI: 10.1007/978-3-031-63751-3_22

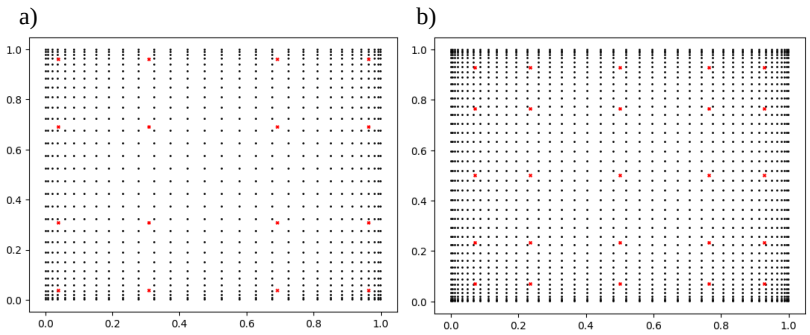

Fig. 5. Two exemplary analyzed combinations of collocation points (in red) and nodes (in black): 4×4 collocation points and 30×30 quadrature nodes (a), and 5×5 collocation points and 40×40 quadrature nodes (b).

Figure 6 illustrates the L_2 norm of the error in solutions on the boundary as a function of the number of introduced collocation points and Gauss quadrature nodes.

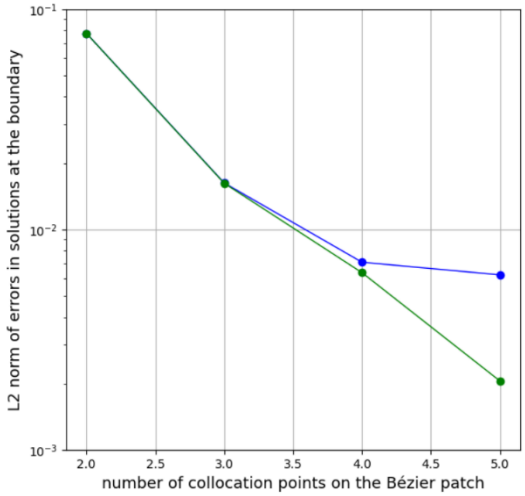

Fig. 6. Influence of the number of collocation points and Gauss quadrature nodes on the accuracy of solutions at the boundary of the problem.

The results again confirm the stability of solutions, even for a more complex domain compared to the first example.

5 Conclusions

The paper demonstrated the possibility of solving PIES without the need to calculate the values of singular integrals. The compiled results indicate a high accuracy of solutions even for a small number of solved algebraic equations. The presented approach

ICCS Camera Ready Version 2024
To cite this paper please use the final published version:
DOI: 10.1007/978-3-031-63751-3_22

can be applied to problems modeled by other differential equations, such as the Navier-Lame or Stokes equations.

References

1. Thomas, J. W. (1998). Numerical partial differential equations: finite difference methods. (volume 22). Springer ScienceBusiness Media New York 1995.
2. Zienkiewicz, O. C., Taylor, R. L., & Zhu, J. Z. (2005). The finite element method: its basis and fundamentals. Elsevier.
3. Brebbia, C. A., Telles, J. C. F., & Wrobel, L. C. (2012). Boundary element techniques: theory and applications in engineering. Springer Science & Business Media.
4. Liu, G. R., & Gu, Y. T. (2005). An introduction to meshfree methods and their programming. Springer Science & Business Media.
5. Zieniuk, E., & Szerszen, K. (2014). The PIES for solving 3D potential problems with domains bounded by rectangular Bézier patches. Engineering Computations, 31(4), 791-809.
6. Zieniuk, E., & Szerszeń, K. (2018). A separation of the boundary geometry from the boundary functions in PIES for 3D problems modeled by the Navier–Lamé equation. Computers & Mathematics with Applications, 75(4), 1067-1094.
7. Telles, J. (1987). A self-adaptive co-ordinate transformation for efficient numerical evaluation of general boundary element integrals. International Journal for Numerical Methods in Engineering, 24(5), 959-973.
8. Miao, Y., Li, W., Lv, J. H., & Long, X. H. (2013). Distance transformation for the numerical evaluation of nearly singular integrals on triangular elements. Engineering Analysis with Boundary Elements, 37(10), 1311-1317.
9. Cerrolaza, M., & Alarcon, E. (1989). A bi-cubic transformation for the numerical evaluation of the Cauchy principal value integrals in boundary methods. International Journal for Numerical Methods in Engineering, 28(5), 987-999.
10. Sladek, V., Sladek, J., & Tanaka, M. (2000). Optimal transformations of the integration variables in computation of singular integrals in BEM. International Journal for Numerical Methods in Engineering, 47(7), 1263-1283.
11. Zhou, H., Niu, Z., Cheng, C., & Guan, Z. (2008). Analytical integral algorithm applied to boundary layer effect and thin body effect in BEM for anisotropic potential problems. Computers & Structures, 86(15-16), 1656-1671.
12. Niu, Z., Wendland, W. L., Wang, X., & Zhou, H. (2005). A semi-analytical algorithm for the evaluation of the nearly singular integrals in three-dimensional boundary element methods. Computer Methods in Applied Mechanics and Engineering, 194(9-11), 1057-1074.
13. Hayami, K., & Matsumoto, H. (1994). A numerical quadrature for nearly singular boundary element integrals. Engineering Analysis with Boundary Elements, 13(2), 143-154.
14. Shiah, Y. C., & Shih, Y. S. (2007). Regularization of nearly singular integrals in the boundary element analysis for interior anisotropic thermal field near the boundary. Journal of the Chinese Institute of Engineers, 30(2), 219-230.
15. Chen, H. B., Lu, P., & Schnack, E. (2001). Regularized algorithms for the calculation of values on and near boundaries in 2D elastic BEM. Engineering Analysis with Boundary Elements, 25(10), 851-876.
16. Sladek, V., Sladek, J., & Tanaka, M. (1993). Regularization of hypersingular and nearly singular integrals in the potential theory and elasticity. International Journal for Numerical Methods in Engineering, 36(10), 1609-1628.

ICCS Camera Ready Version 2024
To cite this paper please use the final published version:
DOI: 10.1007/978-3-031-63751-3_22

17. Zieniuk, E., & Szerszeń, K. (2022). A regularization of the parametric integral equation system applied to 2D boundary problems for Laplace's equation with stability evaluation. Journal of Computational Science, 61, 101658.
18. Szerszeń, K., Zieniuk, E., Bołtuć, A., & Kużelewski, A. (2021). Comprehensive regularization of PIES for problems modeled by 2D Laplace's equation. In International Conference on Computational Science (465-479). Cham: Springer International Publishing.
19. Zieniuk, E., & Szerszeń, K. (2024). Near corner boundary regularization of the parametric integral equation system (PIES). Engineering Analysis with Boundary Elements, 158, 51-67.

ICCS Camera Ready Version 2024
To cite this paper please use the final published version:
DOI: 10.1007/978-3-031-63751-3_22